2007 IEEE International Conference on
Robotics and Automation
Roma, Italy, 10-14 April 2007

An Optical Fiber Proximity Sensor for Haptic Exploration

Sean Walker*, Kevin Loewke†, Michael Fischer*, Carl Liu*, and J. Kenneth Salisbury*
*Department of Computer Science
†Department of Mechanical Engineering
Stanford University
Stanford, CA 94305 USA
{spw, kloewke, mfischer, carlliu}@stanford.edu, jks@robotics.stanford.edu

***Abstract*— This paper presents the design of an optical fiber proximity sensor for haptic exploration with a robotic finger. The sensor uses emitter and receiver optical fiber pairs to measure the intensity of light reflected off surrounding objects in a 2-D workspace. We present the design and construction a 32-point sensor array mounted within a 36 *mm* diameter finger and describe software techniques to process data acquired by an inexpensive web-cam. We experimentally characterize the sensor performance and demonstrate applications for haptic exploration such as pre-contact velocity reduction and non-contact contour following based on object curvature.**

I. Introduction

Much of the dexterous manipulation required in human day-to-day life must be accomplished without visual feedback. Tasks such as getting keys from a pocket, changing an oil filter, or changing a light bulb all require the use of our exquisite touch capabilities. In robotics, however, the current lack of advanced touch sensing techniques presents a major obstacle to the advance of autonomous and dexterous robotic manipulation. This work is part of an effort to develop next generation dexterous robot hands with new capabilities for sensing, active exploration, and manipulation.

In particular, one of the goals of our research is to apply probabilistic techniques [1] to interpret multi-sensory information and model the inherent uncertainty involved with physical manipulation. Accordingly, we have constructed the Probabilistic Manipulation Experiment Table (PMET), as shown in Figure 1, to explore the use of various types of sensors and perceptual methods. The PMET currently contains an instrumented two degree-of-freedom robot designed to push objects in the plane with its 'finger'. The manipulator is controlled by our Probabilistic Robotics Studio (PRS), an interactive design and development studio running Real Time Linux version 3.1 [2] [3].

In this paper we use the PMET and PRS to explore one particular and relatively uncommon perceptual method for robotic manipulation: proximity sensing. Specifically, we present the design and development of an optical fiber proximity sensor (OFPS), as shown in Figure 1. The OFPS has several notable characteristics, including low cost, high sensor density, inherently robust design (as there are no moving parts or mechanical transducers), and high reliability in controlled environments. One of the most powerful advantages of the OFPS over contact-based tactile sensors is the ability to anticipate an approaching object, which can make robots cautious and thus more human-friendly [4]. For the robotic manipulator considered in this paper, we use this proximity information for specific tasks such as pre-contact velocity reduction and smooth non-contact contour following based on object curvature.

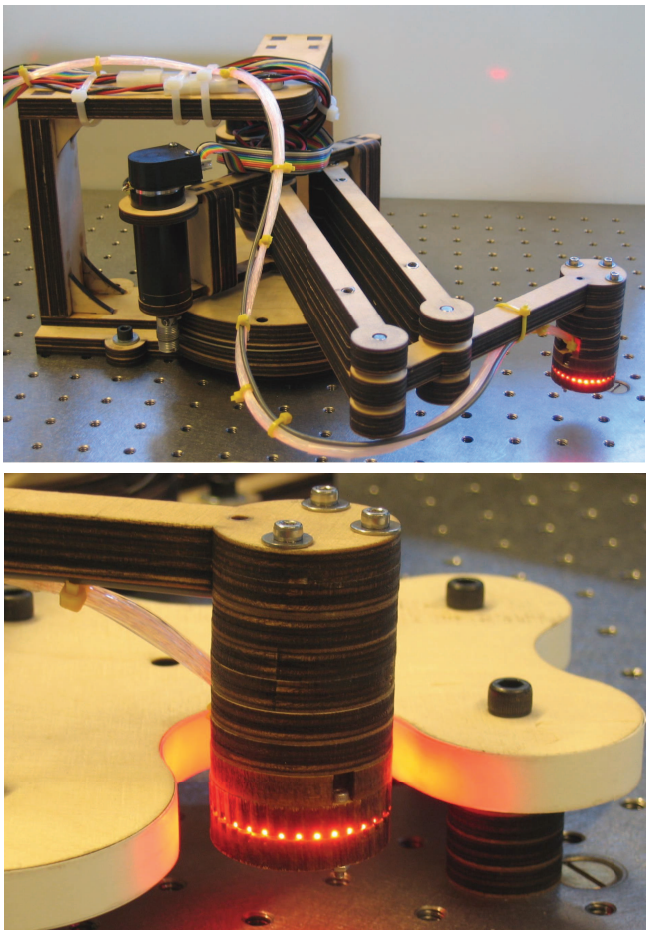

Fig. 1. Probabilistic Manipulation Experiment Table (PMET). The end-effector, or 'finger', is equipped with an optical fiber proximity sensor (OFPS) as well as an embedded accelerometer.

In the following section we discuss previous work related to robot hands, tactile sensors, and optical sensors. We then present the hardware and software development for the OFPS, characterize its performance, and present two experiments which take advantage of its unique capabilities.

II. Previous Work

Early work on robot hands, including the efforts of Okada [5], Salisbury [6], and Jacobsen [7], focused on the design of hands with appropriate kinematics, force controllability, and various add-on sensors. Many of these devices, including more recent hands designs by researchers at DLR [8] [9] were used to support work on grasp planning, object recognition, and grasp gaits.

Tactile sensors are an important element of robot manipulation and their development has been an area of intense research. Grupen summarizes several tactile sensing technologies such as optical sensors, pressure sensors, and vibration sensors [10], and Howe describes several tactile sensor devices and their applications for manipulation [11]. Ellis experimented with methods of using a sensor in both passive and active modes by modulating contact pressure [12]. Debus made an inherently passive pressure sensor active by manually moving it across subjects [13].

There have also been previous efforts towards developing light-based tactile sensors and sensor 'skins' using components such as LEDs, photo-detectors, and optical fibers. Begej provides an overview of such sensors, as well as the development of two optical tactile sensors for a robot gripper and fingertip [14]. Recently, Ohmura described the development of a conformable tactile sensor skin consisting of LEDs/photo-detectors covered by urethane foam [15]. While both of these designs had optical components, they were used to sense pressure rather than proximity.

Proximity sensors such as laser scanners or sonar units have been a foundation of mobile robotics navigation for decades [16] [17]. Yet, very few researchers have applied proximity sensing to manipulation. One prior effort was carried out by Lumelsky who developed a sensitive skin composed of an array of LEDs/photo-detectors wrapped around the arm of a robotic manipulator [4]. Although a novel idea, it would be difficult to implement this sensor for manipulation with a robotic hand or finger due to the low-density of sensing elements (25 mm spacing) and exposed components that are susceptible to impact and shear forces.

In the following section we build upon the sensing techniques developed by Begej and Lumelsky to develop a new optical fiber proximity sensor.

III. Sensor Design

The fundamental principle behind an optical proximity sensor is to measure the intensity of light reflected off an approaching object. Our OFPS was designed specifically for the finger of our robotic manipulator, and has the following notable characteristics:

- Thin optical fibers allow for high spatial density (32 elements within a 36 mm diameter cylinder).
- The sensor is inherently robust as there are no moving parts or mechanical transducers.
- A USB web-cam provides cheap and easily scalable data acquisition.
- Fabrication involves low-cost rapid prototyping techniques for a total cost of under $100.

The design process for developing this sensor resulted in two different versions, as described in the following sections.

A. Version 1

The first version of the sensor, shown in Figure 2, has 16 sensing elements spaced evenly around the circumference of a 36 mm diameter section of the finger. Each sensing element uses an embedded high-intensity LED to generate the source light signal. The LEDs were sanded down to reduce their cross-sectional size to 3.0 mm by 1.5 mm and then polished. The reflected light signal is detected by 1.0 mm diameter, 1.0 m long optical fibers that are routed to a web-cam mounting unit.

At the point of contact near the outer edge, both the LEDs and optical fiber faces are recessed slightly in the groove to ensure that the approaching object will not completely block either the emitter or detector. In order to eliminate unintentional cross-talk between the LEDs and fibers, a piece of reflective tape is used as an isolation layer. The housing unit and web-cam mount were designed in CAD and fabricated out of plywood using a LaserCAMM rapid-prototyping machine that precisely laser-machined both the shape and depth grooves.

This first version of the sensor was designed for proof-of-concept. Accordingly, an emphasis was placed on generating and detecting strong light signals via embedded LEDs and relatively large-diameter fibers. In order to reduce component size and increase the spatial density, we developed a second version that uses thinner fibers and a more efficient method for illumination.

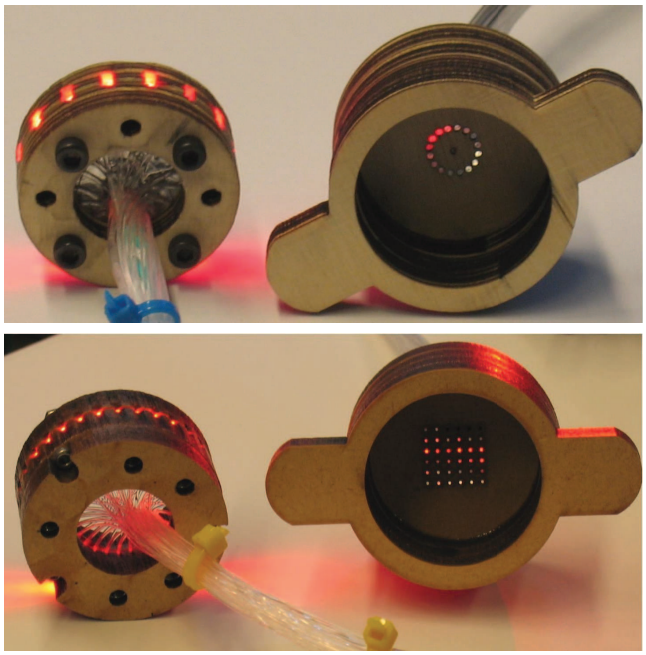

Fig. 2. Version 1 (top) and Version 2 (bottom) of OFPS with web-cam mounting units.

B. Version 2

The second version of the sensor, shown in Figure 2, has 32 sensing elements again spaced evenly around the circumference of a 36 mm diameter section of the finger. Each sensing element consists of a pair of 0.5 mm diameter, 1.0 m long optical fibers that transmit both the source signal and detected signal. The light source is a remotely located 3-watt Luxeon 'Power LED', and the detected signal is fed to a web-cam mounting unit.

The housing unit for the second sensor is similar to the first sensor with additional features such as recessed and flared grooves that maintain the gap between the approaching object and sensor while allowing a wide acceptance angle for the fibers. An exploded view of the internal structure is shown in Figure 3. This second version of the sensor was used for all subsequent analysis presented in this paper.

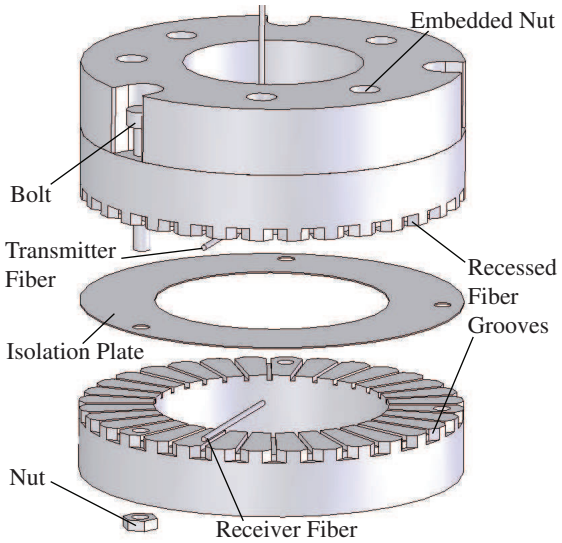

Fig. 3. Exploded view of Version 2 of OFPS. Components are shown for only 1 of the 32 sensing elements. Bolts are used for securing unit, and embedded nuts are used for attaching to robot finger.

IV. Software

Our software implementation was integrated with the PRS using an inexpensive Labtec webcam (a Logitech Quickcam Express clone) for data acquisition. In order to get tight control over image parameters we directly interfaced with the qc-usb Video4Linux driver [18]. After disabling automatic exposure control, we adjusted the camera to use a very short exposure time and a small gain since the proximity sensor signals were quite bright. The short exposure time allowed us to achieve a very fast frame rate of 48 frames per second using a window size of 128 x 128 pixels.

The raw camera signal is shown in the lower right corner of Figure 4. Each fiber produces a circle of light on the camera sensor. Our software locates each of these light circles through calibration, processes each group of lighted pixels to reduce noise and interference from other light sources, and sums the resulting group of pixel intensities to produce a sensor signal. The next two sections describe the calibration and noise reduction procedures.

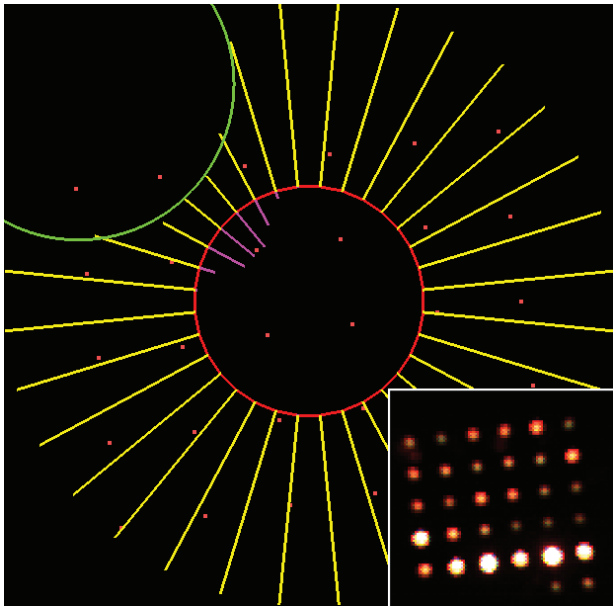

Fig. 4. Proximity signal display and raw camera image (inset).

A. Calibration

Calibration consists of two steps. The first step calibrates the location of each sensor allowing the camera mount to be imprecise as long as the receiver fibers are mounted in a uniform grid. Using a longer exposure setting to brighten the signals, the upper left, upper right, and lower right circles are located using a simple scanning procedure. Then the center of each circle is found by computing a position average weighted by intensity. The resulting three points in camera space can be used to estimate the position, rotation, and scale of the grid of points with a high degree of accuracy.

The second step of calibration is to determine the minimum and maximum intensity for the summed pixels at each sensor location. To do this, the finger traces around a circular object, thereby allowing each sensor to get both the maximum and minimum reflected light. These values are used to normalize the signal between 0 and 1.

B. Noise Reduction

An important challenge of visible light proximity sensors is rejecting light noise from outside sources. The low camera gain and short exposure time makes this easier because the signal to noise ratio is relatively high. In our early experiments we found that light from nearby windows caused noticeable interference in the signal. We explored several options to reduce noise and found the two most successful methods are blinking the light source and color-keying.

The ideal method to reduce light interference is blinking the light source. If the light source is precisely blinked at half the frame rate the difference between on and off frames will be the proximity signal. Theoretically you would still have the same number of signal measurements simply

by comparing each frame to the previous one in order to determine a signal. In practice, we found that this introduced artifacts in the camera signal and it was very difficult to synchronize the camera capture with the illumination.

Instead, since we were using a full color camera, we decided to use the color of the light to differentiate between the signal S and noise. Since the CMOS camera is based on a Bayer pattern [19] we restricted computations to those pixels corresponding to red filters and interpolated the nearby green and blue values (this prevents spatial signals from leaking into the color domain). Experimentally we determined that the red ($625\ nm$) Luxeon LED produced approximately 2 units of green G and 1 unit of blue B for each unit of red R. Using the assumption that light noise from the surrounding room will generally be white ($R = G$), solving for the signal gives us $S = (R - G) * (4/3)$. If $R < G$ then we assume $S = 0$.

The dynamic range of the Labtec camera is quite low, however, and it is relatively easy for the signal to cause R (and sometimes G) to saturate. Generally, noise alone is not able to saturate the sensor, but noise can produce errors even when the signal is relatively large. So, when the red channel saturated we used the signal $S' = (G - B) * 8$ averaged with the red-green difference to estimate the signal. While far from mathematically rigorous, we found it cleaned up the signal and reduced noise.

V. Sensor Characteristics and Performance

A. One-Point

Our first step towards characterizing the OFPS was to isolate a single emitter and receiver pair. Using an automatic script the finger approached a flat surface (to determine the relationship between the distance and the raw signal) and then scanned the object sidewise (to measure the relationship between the angle of the material and the raw signal).

Figure 5 depicts the relationship between the raw signal and the distance for several materials. All materials produce a similar curve that is close to exponential with bright objects visible over $5\ cm$ away. We found that a 3^{rd} degree polynomial in logarithm space produced a good fit with small errors in areas of very large or very small distances. As the sensor signal gets small, however, the noise due to the camera causes a larger relative signal noise in the distance domain.

Figure 6 depicts the normalized intensity of the sensor in relation to the angle of the surface. An angle of zero corresponds to the surface placed exactly perpendicular to the sensor. Each value is normalized based on the distance from the sensor to the surface (along the baseline of the sensor). As shown, objects with shinier surfaces result in a sharper drop-off as the angle increases. The ideal surface is a bright diffuse surface such as paper which will result in a strong signal almost totally independent of surface angle. The worst surface for an optical proximity sensor would be very dark (resulting in poor sensitivity) or very shiny (resulting in very angle-sensitive readings).

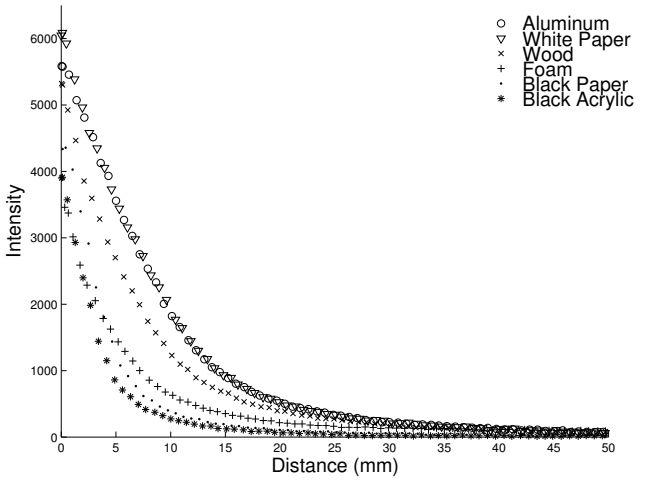

Fig. 5. Distance vs. proximity intensity for a variety of materials.

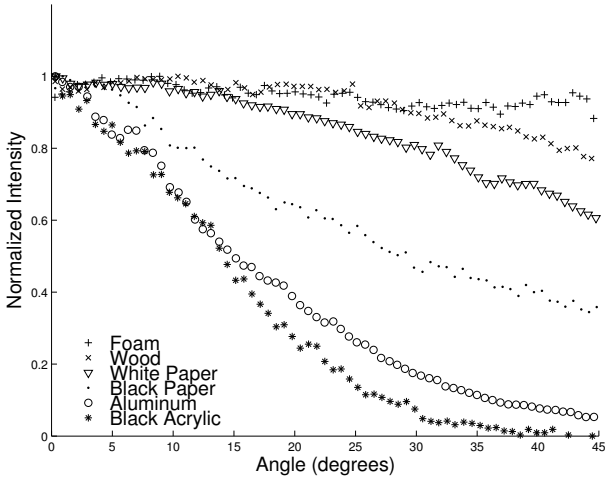

Fig. 6. Angle vs. normalized proximity intensity for a variety of materials.

B. Multiple-Points

Once we characterized a single sensor, we began running experiments using all 32 sensors on the fingertip. An important advantage of the OFPS described in this paper is the ability to acquire multiple readings in parallel.

Enabling all sensors causes more light to reach each receiver because nearby emitters will also contribute light to the sensor. Despite this extra light, the general shape of the sensor distance vs. signal is the same. To avoid calibrating each sensor, we made the assumption that the normalized sensor value (between 0 and 1) would react approximately the same for each emitter/receiver pair. Using a linear fit to the logarithm of the raw signal gave values that were accurate enough for our experiments.

The radial lines inside the circle in Figure 4 correspond to the sensor value while the lines outside the circle correspond to the distance computed using the calibrated curve. Since the scale of the fingertip and distance calibration is known, the result is a cloud of nearest object measurements around the current fingertip location. These measurements tend to

have more noise and error at longer distances and we found it useful to clip all distances beyond a cutoff distance (d_{max}, $3\ cm$ in our experiments). By ignoring the noise prone region of large distances we maintained a set of reliable measurements in the immediate area around the fingertip.

While the simplest use of this sensor is just to identify the receiver with the closest object, the advantage of a multi-point OFPS is the large amount of distance measurements read in at the same time. There are many methods of modeling the physical world around the fingertip, and we took the first step by fitting the distance measurements to a circle as shown in Figure 4. To fit a circle, we used the Levenberg-Marquardt non-linear least squares algorithm to compute the parameters of a circle through the measurements around the minimum distance measurement. This technique worked very well as long as the object being sensed approximated a circular arc.

C. External Coverings

An air gap is not always the ideal situation for providing emitter and receiver overlap. Many manipulators require a smooth contact surface or even a compliant surface that can conform to the manipulated objects (much like the skin of humans). OPFSs could be used in these situations but care must be taken to ensure a suitable quantity of light is able to leave the emitter, bounce of the object, and return to the detector.

In our early experiments we found that transparent materials such as glass or clear acrylic work well for producing a gap for the light to spread and reflect in. In order to test a clear compliant material we molded a thin piece of Dragon Skin, a durable silicone rubber made by Smooth-On [20]. We stretched a thin layer of Dragon Skin over the fingertip and plotted distanced vs. signal for white paper in Figure 7. Although there is a significant amount of reflection interference, the signal is still usable out to about $1\ cm$. We believe the signal would improve significantly if we had been able to place the transparent covering flush with the fiber ends (which was not part of our original design).

VI. Experiments

In this section we describe two experiments we performed to determine the strengths and weaknesses of the OFPS.

A. Proximity Detection to Avoid Collisions

One of our first tests was to see how quickly the OFPS could sense an object and avoid contact with it. For this experiment we used the raw proximity signal to achieve the highest sensitivity.

In the experiment, the PMET finger moved toward an object mounted on an ATI force sensor at a constant velocity. When the OFPS detected the object the finger was commanded to move away. If the finger impacted the force sensor we called the test a failure, but if it did not hit the force sensor, we called it a success. We started at a low velocity and ran the test at increasingly higher velocities until all 20 repetitions were failures.

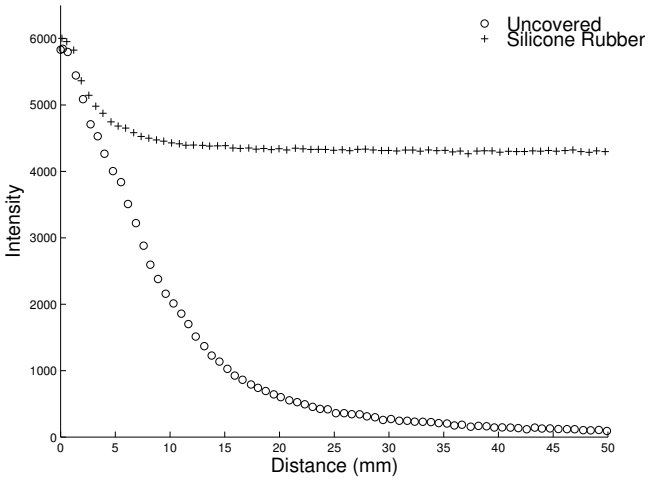

Fig. 7. Distance vs. proximity characteristics of Dragon Skin (silicone rubber) covering.

We found that the finger could avoid hitting the object 100% of the time at velocities lower than $0.8\ m/s$. Likewise, the experiments failed 100% of the time above $1\ m/s$, with a relatively rapid drop-off between the speeds.

This experiment depends on many different factors, including servo loop update rate, camera frame rate, and dynamic properties of the robot. Obviously, with a higher camera frame rate or a more rigid robot the detection and reverse in direction could occur more quickly. In our estimation, the dynamics of the robot play the biggest part in the ability to stop in time. The important thing to note is the ability to avoid contact with objects well before contact is made is enabled exclusively by the proximity sensor.

B. Following a Contour

The parallel nature of the OFPS allows the shape and curvature of objects to be scanned by the finger before any contact is made. Our second experiment was to trace around an object without touching it and acquire a cloud of points on the surface of the object as shown in Figure 8. These point clouds could easily be used in probabilistic mapping functions. For this paper, we focus on techniques used to trace a smooth path around the object without touching it.

The object we chose to trace around (shown in the bottom part of Figure 1) is approximately $20\ cm$ on each side with a curved surface and both convex and concave features. The simplest way to track around the object is to move the fingertip in small (approximately $2\ mm$) straight-line steps tangent to the object. Initially, we determined these steps by choosing a direction normal to the sensor element which was closest to the object. In addition, adjustments to the step were made towards or away from the object based on the distance between the fingertip and the object. The path the finger took is shown in Figure 8. Note that the center of the fingertip is plotted which causes the extra $18\ mm$ gap (for the finger radius) in addition to the $1\ cm$ edge-following distance.

While the tangent to closest point method produces a good map of the object, the path of the finger is not very smooth.

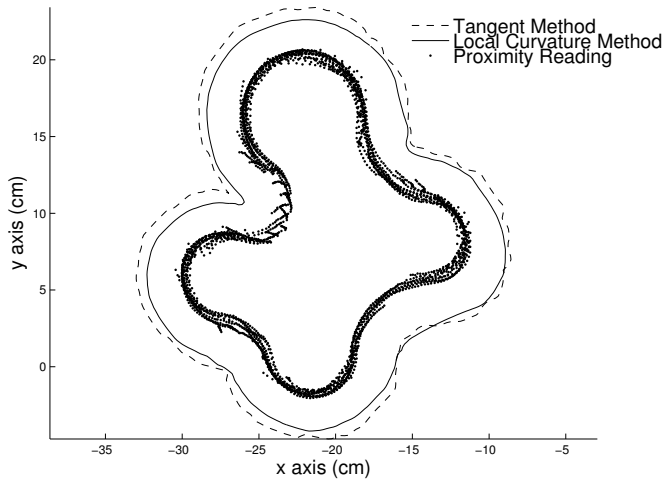

Fig. 8. Contour mapping results for single pass around the object. The proximity readings correspond to the local curvature method.

Accordingly, we decided to use the local curvature of the object to plan each new straight-line step. To do this, we took the closest sensor to the object and fit a circle to the nearby distance measurements as described in the previous section. Then, we used the closest point on the circle to the fingertip to estimate the next step along the circle and the corresponding finger location. The end result is the smoother path shown in Figure 8.

VII. Conclusion

In this paper we have presented a new optical fiber proximity sensor which provides a reliable and useful alternative to conventional pressure-based tactile sensors. In addition to presenting the construction and performance characteristics we have demonstrated the use of such a sensor in practice.

A parallel proximity sensor, while insensitive to force, has a number of advantages over a conventional capacitive or resistive pressure sensor. First, because it has no mechanical parts, it is less likely to break or wear out. Second, the ability to sense objects before contact is made and even sense the shape of the object allows control algorithms impossible with a tactile sensor. Third, the use of thin optical fibers allows for high sensor density. Finally, fabrication is relatively easy and costs less than $100 in total.

Like all sensors, the OFPS has limitations. First, small, narrow objects will cause only small activation of the sensor and confuse it. Second, dark or highly reflective objects will confuse the sensor since the response is very much dependent upon the material. Beyond restricting the light wavelength (such as narrow band infrared), a good solution would be to combine a series of measurements along with positioning information similar to [21]. The appropriate technique, if provided with enough points, should be able to estimate the shape and reflectivity of the objects.

There remains a lot that we would like to explore with this class of proximity sensors. Future work on this project will apply probabilistic algorithms such as particle filters to the processing of the proximity data and explicitly model the noise inherent in the sensor. In addition, there are some more advanced structures to the sensor which we would like to explore. For instance, it would be interesting to learn if optical fibers could be embedded into a flexible skin with special fittings to orient the sensitive area normal to the skin. Another possibility is to locate a CCD chip and microcontroller inside the fingertip to eliminate long fiber runs.

Ultimately we envision a multi-fingered hand suitable for grasping and manipulation which uses bands of OFPSs located on each finger link.

VIII. Acknowledgements

This work was supported by NSF Grant number 0535289 and an NSF Graduate Research Fellowship.

References

[1] S. Thrun, "Probabilistic algorithms in robotics," *AI Magazine*, vol. 21, no. 4, pp. 93–109, 2000.
[2] [Online]. Available: http://www.rtlinuxfree.com/
[3] V. Yodaiken and M. Barabanov, "A real-time linux," in *Proceedings of the Linux Applications Development and Deployment Conference (USELINUX)*, Anaheim, CA, Jan. 1997.
[4] V. Lumelsky, M. Shur, and S. Wagner, "Sensitive skin," *IEEE Sensors Journal*, vol. 1, no. 1, pp. 41–51, 2001.
[5] T. Okada, "Object handling system for manual industry," *IEEE Transactions on Systems, Man, and Cybernetics*, vol. 9, no. 2, pp. 79–89, 1979.
[6] M. Mason and K. Salisbury, *Robot Hands and the Mechanics of Manipulation*. MIT Press, 1985.
[7] S. Jacobsen, E. Iversen, D. Knutti, R. Johnson, and K. Bigger, "Design of the utah/mit dextrous hand," in *Proc. IEEE International Conference on Robotics and Automation*, 1986, pp. 96–102.
[8] L. Biagiotti, F. Lotti, G. Palli, P. Tiezzi, G. Vassura, and C. Melchiorri, "Dlr hand ii: Experiments and experiences with an anthropomorphic hand," in *Proc. IEEE International Conference on Robotics and Automation*, Taipei, Taiwan, 2003.
[9] C. Borst, M. Fischer, S. Haidacher, H. Liu, and G. Hirzinger, "Development of ub hand 3: Early results," in *Proc. IEEE International Conference on Robotics and Automation*, Barcelona, Spain, 2005.
[10] R. Grupen, T. Henderson, and I. McCammon, "A survey of general-purpose manipulation," *The International Journal of Robotics Research*, pp. 38–62, 1989.
[11] R. Howe, "Tactile sensing and control of robotic manipulation," *Journal of Advanced Robotics*, vol. 8, no. 3, pp. 245–261, 1994.
[12] R. Ellis, "Extraction of tactile features by passive and active sensing," *SPIE Intelligent Robots and Computer Vision*, vol. 521, pp. 289–295, 1984.
[13] T. Debus, P. Dupont, and R. Howe, "Contact state estimation using multiple model estimation and hidden markov models," *International Journal of Robotics Research*, vol. 23, no. 4-5, pp. 399–413, 2004.
[14] S. Begej, "Planar and finger-shaped optical tactile sensors for robotic applications," *IEEE Journal of Robotics and Automation*, vol. 4, no. 5, pp. 472–484, 1988.
[15] Y. Ohmura, Y. Kuniyoshi, and A. Nagakubo, "Conformable and scalable tactile sensor skin for curved surfaces," in *Proc. IEEE International Conference on Robotics and Automation*, Orlando, Florida, May 2006, pp. 1348–1353.
[16] S. Thrun, W. Burgard, and D. Fox, "A real-time algorithm for mobile robot mapping with applications to multi-robot and 3D mapping," in *Proceedings of the IEEE International Conference on Robotics and Automation (ICRA)*. San Francisco, CA: IEEE, 2000.
[17] A. Elfes, "Sonar-based real-world mapping and navigation," in *Proceedings of the IEEE Journal of Robotics and Automation*, vol. RA-3, no. 3, 1987, pp. 249–265.
[18] [Online]. Available: http://qce-ga.sourceforge.net/
[19] US Patent 3,971,065.
[20] [Online]. Available: http://www.smooth-on.com/
[21] M. A. Garcia and A. Solanas, "Estimation of distance of planar surfaces and type of material with infrared sensors," in *Proceedings of the 17th International Conference on Pattern Recognition*, 2004.